

Phase Diagrams and Sublimation Enthalpies of Model $C_{n \geq 60}$ Fullerenes: A Comparative Study by Computer Simulation

Fernando M. S. Silva Fernandes,* Filomena F. M. Freitas, and Rui P. S. Fartaria

Laboratory of Molecular Simulation and CECUL, Department of Chemistry and Biochemistry, Faculty of Science, University of Lisboa, Rua Ernesto de Vasconcelos, Bloco C8, Piso 3, 1749-016 Lisboa, Portugal

Received: August 19, 2002; In Final Form: October 21, 2002

A comparative study, strictly by computer simulation, of the phase diagrams and sublimation enthalpies of model $C_{n \geq 60}$ fullerenes is presented. Gibbs ensemble and Gibbs–Duhem integration Monte Carlo simulations were carried out with the effective potentials of Girifalco. The triple-point properties were determined by a direct method recently proposed by us. It is based on the behavior of the Gibbs ensemble simulations at the lowest temperature limit, and it does not involve free-energy calculations or any other theoretical approach. According to the present results, the liquid phases of the studied fullerenes (C_{60} , C_{70} , C_{76} , and C_{84}) extend over ~ 450 K. No sign of liquid supercooling was observed. The triple-point temperatures increase from C_{60} to C_{84} . This and the simultaneous effect of molecular size cause a relative dislocation of the phase diagrams to higher critical temperatures and lower densities. The simulated enthalpies of sublimation increase from C_{60} to C_{84} , and they are in very good agreement with the available experimental data. It is suggested that at least the predicted triple-point properties should approach those of real fullerenes. There is a strong correlation between the phase properties and the details of the interaction potentials, clearly reflected in the relative location of the phase diagram and enthalpy curves. On the whole, the simulated results are in good accordance with those recently reported by Abramo et al. (Abramo, M. C.; Caccamo, C.; Costa, D.; Pellicane, G. *Europhys. Lett.* **2001**, *54*, 468) from a combination of simulation, modified hypernetted chain (MHNC) theory, and a kind of “corresponding states” rule and confirm the consistency of the MHNC theoretical approach. The reduced properties, which also include the critical- and triple-point pressures as well as the sublimation enthalpies, confirm that some kind of corresponding states rule may be established for fullerenes. On the basis of that, the enthalpy of sublimation of C_{96} is predicted.

1. Introduction

Computer simulation in statistical mechanics is a powerful tool for the production of quasi-exact results for a molecular model. It serves two main purposes. On one hand, it is able to test a theoretical approach unambiguously. On the other hand, it can confirm, correct, or reject a given model against experimental evidence. Therefore, if it is possible to study a molecular model strictly by computer simulation, then we presumably get the “two sides of the coin”. This is the spirit of the present article.

In a recent letter, Abramo et al.¹ reported a systematic study of the phase behavior of model fullerenes based on Girifalco’s potential (GP).² Monte Carlo simulations were combined with the modified hypernetted chain (MHNC) theoretical approach to obtain the vapor–liquid coexistence curve, the freezing line, and the critical- and the triple-point temperatures and densities of C_{70} . Structural and dynamic properties were also calculated in the predicted liquid pocket, showing that the results are consistent with a normal liquid state. No sign of liquid supercooling was observed. From a kind of “corresponding states” rule for fullerenes, the critical- and triple-point temperatures and densities for C_{76} , C_{84} , and C_{96} were predicted. They concluded that the model fullerenes have liquid phases that

extend over almost 500 K, a temperature range considerably wider than the one found for C_{60} (~ 90 K).

The mentioned temperature interval of ~ 90 K for the existence of liquid C_{60} seems, however, to be a matter of choice between two sets of apparently conflicting triple-point data: one, from free-energy Monte Carlo calculations,³ that estimates a triple-point temperature considerably higher than the other based on simulation combined with the hypernetted mean spherical approximation and the modified hypernetted chain theories.^{4–7}

In recent articles^{8,9} based on two different simulation approaches to estimate the triple point and using a first-principles interaction potential (PRP)¹⁰ and Girifalco’s potential (GP), we have shown that both interaction models for C_{60} are able to reproduce two sets of triple point properties: one, in which the triple point is approached from high temperatures, agrees with free-energy-based calculations; the other, in which the triple point is approached from lower temperatures, is in accordance with the findings of HMSA and MHNC theoretical approaches. The high-temperature set indicates that the liquid phase for C_{60} extends over ~ 100 K, and the low-temperature one, that the liquid extends over ~ 450 K. Moreover, we suggested that the high-temperature results correspond to local minima of the Gibbs free energy, whereas the low-temperature results correspond to the free-energy global minima. Then, from the low-temperature triple points, we simulated the vapor–solid and liquid–solid

* To whom correspondence should be addressed. E-mail: fsilva@fc.ul.pt.

TABLE 1: Parameters of Girifalco's Potential

	R/nm	R_0/nm	$-\epsilon/k_B$	$\alpha/10^{-15}\text{erg}$	$\beta/10^{-18}\text{erg}$
C_{60}	0.71	0.9599	3218	74.94	135.95
C_{70}	0.762	1.011	3653	66.7	79.23
C_{76}	0.7991	1.048	3808	59.2	52.87
C_{84}	0.8401	1.0890	4081	53.56	35.42

coexistence properties. The enthalpies of sublimation, in particular, are in very good agreement with the available experimental data.

The low-temperature triple-point properties were determined by a direct approach recently proposed by us.¹¹ It is based on the behavior of the Gibbs ensemble vapor–liquid simulations at the lowest temperature limit, and it does not involve free-energy calculations or any other theoretical approach.

The main objectives of the present work are (i) to trace the whole phase diagrams of C_{70} , C_{76} , and C_{84} on the basis of GP using the same techniques as in our previous articles for C_{60} , that is, strictly by computer simulation; (ii) to compare the simulated critical- and triple-point properties with the ones reported by Abramo et al.¹ for the same potential models, which will be an independent test of the reliability of the MHNC theory used by those authors and of their suggestion of a corresponding states rule for fullerenes; (iii) to compare the predicted enthalpies of sublimation with the available experimental data, which will assess the reality of the present models; and (iv) to correlate the simulated results with the main characteristics of the potential models, which is directly connected to the possibility of establishing a corresponding states rule for fullerenes. To this end, we also include some of our results for C_{60} reported elsewhere.⁹

In the next section, we present the potential model and the computational details. The results are shown and discussed in sections 3 and 4. The final section contains the conclusions of this work.

2. Interaction Potentials and Computational Details

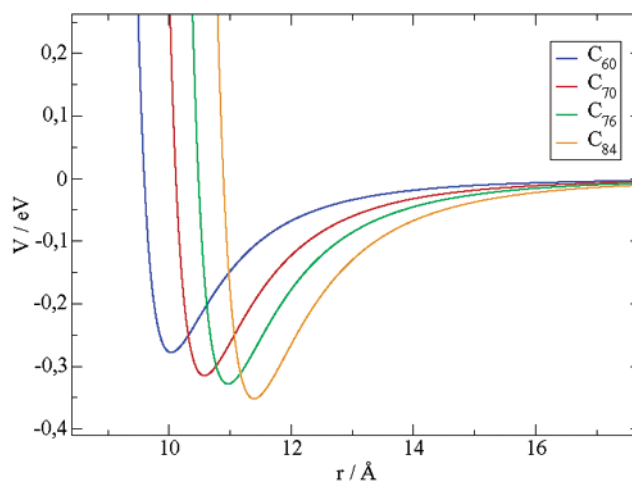
The potential of Girifalco (GP)² has the form

$$V(r) = -\alpha \left[\frac{1}{s(s-1)^3} + \frac{1}{s(s+1)^3} - \frac{2}{s^4} \right] + \beta \left[\frac{1}{s(s-1)^9} + \frac{1}{s(s+1)^9} - \frac{2}{s^{10}} \right] \quad (1)$$

where $s = r/R$, $\alpha = N^2 A / 12 R^6$, and $\beta = N^2 B / 90 R^{12}$. N and R are, respectively, the number of carbon atoms and the diameter of the fullerene molecules; $A = 32 \times 10^{-60} \text{ erg cm}^6$ and $B = 55.77 \times 10^{-105} \text{ erg cm}^{12}$ are constants entering the Lennard-Jones 12–6 potential through which two carbon sites on different sphericalized molecules are assumed to interact. The specific parameters for the different fullerenes, presented in Table 1, are the ones given by Abramo et al.¹ and Zubov et al.¹²

GP is a very useful interaction potential since it can be easily adapted to fullerenes with different numbers of carbon atoms. In addition, our present and previous work suggests that it is also a good effective potential, at least for some phase properties in the lower temperature limit. Indeed, it is able to reproduce very well the experimental enthalpies of sublimation of the studied C_n fullerenes.

Figure 1, displays the potentials for the fullerenes analyzed in this work. They are all very hard and short-ranged, decaying rapidly to zero for distances greater than $2R_0$ (R_0 is the effective diameter of the molecules). The repulsive parts have similar

**Figure 1.** Girifalco's potentials.

trends, with the location of R_0 reflecting the molecular size. Also, the potential depths increase significantly from C_{60} to C_{84} . It is important to point out these aspects regarding the discussion in the next sections.

The potentials were truncated at half of the simulation box lengths. As these distances were always greater than $2R_0$, long-range corrections were not included. Nonetheless, taking into account the study of Hasegawa and Ohno,¹³ we have verified that the used truncation distances have negligible effects on the phase diagrams. The usual cubic periodic boundary conditions were applied.

The vapor–liquid coexistence curves were obtained by Gibbs ensemble Monte Carlo (GEMC) simulations.^{14,15} The first point was set up by placing the molecules in face-centered-cubic (fcc) lattices with 256 molecules in each box (cubic box 1 and box 2) at appropriate densities and running a convenient number of cycles for the complete relaxation of the system. The other points were calculated starting from fcc lattices with 256 molecules in each box at the equilibrium densities of the previous runs. Equilibration runs with 3000–10 000 cycles were followed by 5 independent production runs with 20 000–40 000 cycles each. A GEMC cycle consisted of random displacements of the molecules in each box by considering the boxes independently, by a random rearrangement of the volume of each box in such a way that the total volume remains constant, and by using a number of trials to transfer a molecule virtually from one box to another. The virtual exchange of particles is performed as follows. One of the two boxes is chosen, with equal probability, to receive one particle. Suppose it is box 1. Then, simultaneously in box 2, a randomly chosen particle is destroyed. Thus, the total number of particles in the system remains constant. The joint probabilities of creating/destroying a particle and of the volume changes are given elsewhere.^{14–16} It turns out that these probabilities are explicitly independent of the pressures and chemical potentials. Therefore, there is no need to specify the pressures and chemical potentials in GEMC simulations. Even so, we have always calculated them (from the virial theorem and the particle insertion method, respectively) to verify the thermodynamic stability of the vapor–liquid equilibrium. Additionally, the analysis of the probability plots, recommended by Frenkel and Smit,¹⁶ was also carried out in some simulations.

The liquid–solid and vapor–solid coexistence curves were obtained by the Gibbs–Duhem integration Monte Carlo (GDIMC) method.^{17–19} It consisted of successive and simultaneous NpT simulations in two boxes (each containing 256 molecules) combined with a predictor–corrector scheme to estimate (from

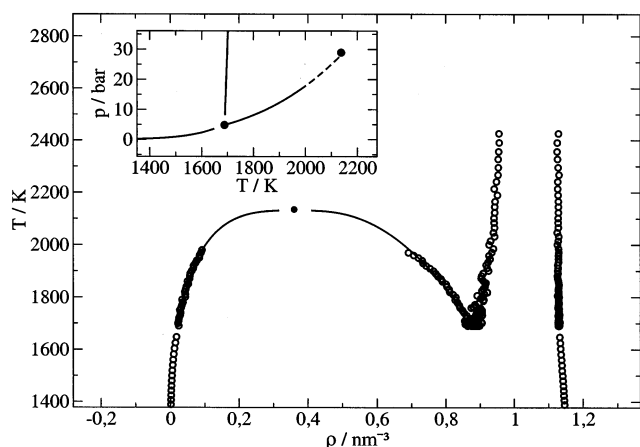


Figure 2. Temperature–density and pressure–temperature (inset) phase diagrams of C_{70} .

the Clapeyron equation) the temperature as a function of pressure for the next point along the coexistence line. The coupling procedure described by Kofke¹⁷ was applied in some calculations. Similar statistics to the GEMC simulations were also carried out. Also, in GDMC calculations, the chemical potentials do not explicitly appear in the final formulation of the method.

Despite the explicit absence of the chemical potentials in Gibbs MC simulations, the powerful hand of the free energy is always present, however invisible. Thus, those simulations should ultimately be equivalent to the so-called free-energy calculations referred to in the abstract and in the body of the present article. The heart of the matter in such calculations is the explicit determination of the free energies for interacting systems from the well-known free energies of the ideal gas and the Einstein crystal.¹⁶

An important issue in fluid–solid simulations by the GDMC method is the definition of the starting state to initiate the integration of the Clapeyron equation. In the present work, we defined that point through the approach recently proposed by us.¹¹ The full computational details of the method can be seen in the original article. A discussion of the differences between our approach and another alternative proposed by Agrawal and Kofke^{18,19} was presented elsewhere.^{8,9} In short, the method consists of decreasing the temperature of the GEMC vapor–liquid equilibrium by small steps ($\Delta T \approx 10$ K) until a temperature is reached below which the liquid phase is not stable anymore. The system readily assumes a vapor–solid configuration, that is, spontaneous freezing is detected in the high-density box. Those values of the temperature, densities, configurational energies (just before and after freezing), and vapor pressure are taken as an estimate of the triple-point properties. From that point, we successively calculated the liquid–solid lines by increasing the temperature and the vapor–solid lines by decreasing the temperature. We should mention that, if the conditions of the respective computational algorithm

TABLE 3: Relative Chemical Potentials for the Fluid–Solid Coexistence of C_{70}

T/K	fluid $\Delta(\beta\mu)$	solid $\Delta(\beta\mu)$
2501	0.00	0.00
2267	−2.34	−2.34
2084	−4.24	−4.25
1959	−5.73	−5.74
1872	−6.85	−6.87
1812	−7.67	−7.68
1771	−8.25	−8.27
1743	−8.65	−8.67
1725	−8.93	−8.95
1712	−9.13	−9.14
1704	−9.26	−9.27
1698	−9.35	−9.36
1694	−9.41	−9.42
1691	−9.45	−9.46
1690	−9.46	−9.48

are fulfilled, the method does not lead to supercooling of the liquid and it is able to determine the triple-point temperature in a very narrow interval (~ 10 K for fullerenes), within the maximum error usually reported for that property. Moreover, the solid generated by the spontaneous freezing is a quasi-perfect, not defect-rich, face-centered-cubic lattice.

To test the reliability of the fluid–solid simulations, we calculated, from the raw data for each phase, the relative chemical potentials $\Delta(\beta\mu)$ by applying a simple trapezoidal rule to the Gibbs–Duhem equation:

$$d(\beta\mu) = h d\beta + \beta p/\rho d \ln p \quad (2)$$

where $h = u + p/\rho$ is the molar enthalpy and $\beta = 1/k_B T$.

The critical temperatures and densities were estimated by fitting the vapor–liquid data to the laws of rectilinear diameters and order-parameter scaling²⁰ with a critical exponent of ~ 0.33 . The pressures were fitted to the Clapeyron equation. The final triple-point properties were assessed by fitting the fluid–solid raw data and intersecting the vapor–liquid lines with the freezing lines.

3. Phase Diagrams

Figure 2 displays the temperature–density and pressure–temperature phase diagrams of C_{70} . Table 2 presents numerical data for the vapor–liquid equilibrium, and Table 3, the relative chemical potentials for the fluid–solid equilibrium.

The equality of the pressures and chemical potentials, within the error bars, of the vapor–liquid simulations suggests good thermodynamic stability for this region of the phase diagram. Regarding the relative chemical potentials of the fluid–solid equilibrium, no error bars were determined. Even so, their coincidence in both phases is remarkable, showing the consistency of the simulations.

TABLE 2: Vapor–Liquid Coexistence of C_{70} ^a

T/K	ρ_V/nm^{-3}	ρ_L/nm^{-3}	p_V/bar	p_L/bar	$-\mu_V/10^{-13}\text{erg}$	$-\mu_L/10^{-13}\text{erg}$
1980	0.091(0.005)	0.667(0.021)	16.83(0.54)	18.24(2.81)	8.26(0.05)	8.33(0.12)
1920	0.067(0.003)	0.742(0.006)	13.09(0.41)	12.03(3.03)	8.49(0.05)	8.58(0.12)
1890	0.057(0.003)	0.771(0.004)	11.45(0.50)	10.41(2.05)	8.63(0.08)	8.55(0.31)
1800	0.043(0.002)	0.829(0.004)	8.47(0.36)	9.73(2.93)	8.78(0.08)	8.51(0.20)
1770	0.033(0.002)	0.839(0.005)	6.76(0.40)	7.28(1.90)	9.06(0.12)	9.10(0.67)
1710	0.024(0.002)	0.865(0.005)	4.88(0.31)	5.76(2.10)	9.37(0.14)	8.94(0.27)
1690	0.024(0.000)	0.882(0.004)	4.85(0.07)	4.55(4.71)	9.26(0.02)	9.26(0.27)

^a Densities ρ , pressures p , and chemical potentials μ . The numbers in parentheses are rms deviations calculated from five independent runs with 20 000 MC cycles each.

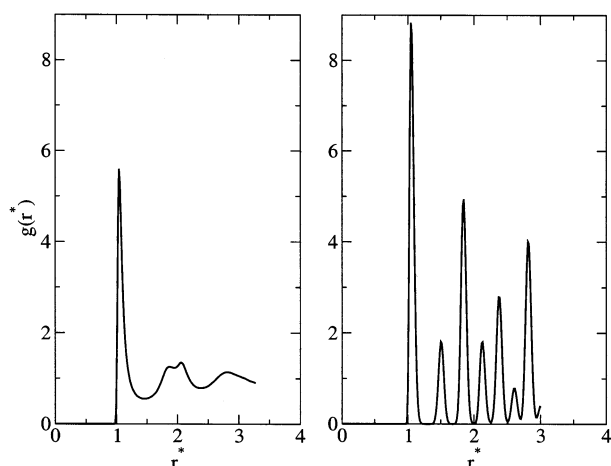


Figure 3. Radial distribution functions for the liquid–solid coexistence of C_{70} (1700 K, near the triple point).

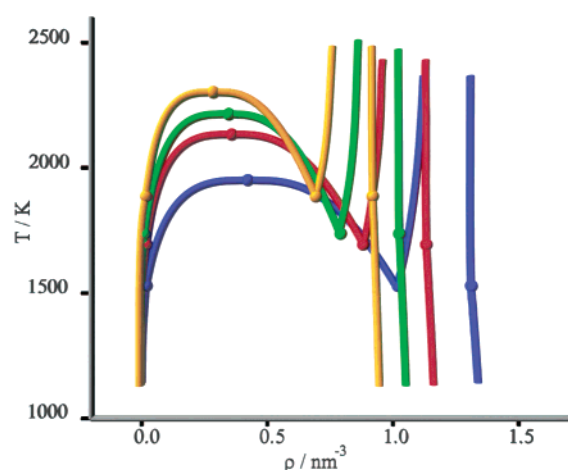


Figure 4. Temperature–density phase diagrams: C_{60} , blue; C_{70} , red; C_{76} , green; and C_{84} , orange.

Figure 3 shows the radial distribution functions for the liquid–solid coexistence near the triple point of C_{70} . They indicate the usual behavior of a liquid and a face-centered-cubic solid lattice, respectively. The shoulders in the second peak of the liquid function, also reported and discussed for C_{60} ,^{4,8,9} indicate the presence of solid or glasslike clusters.

Figure 4 displays the temperature–density phase diagrams for C_{60} , C_{70} , C_{76} , and C_{84} obtained by fitting the simulation raw

data. Table 4 contains the respective numerical results for critical- and triple-point properties as well as some results recently obtained by Abramo et al.¹ The results for C_{60} have been reported elsewhere.⁹

All of the studied model fullerenes present liquid pockets that extend over ~ 450 K. No liquid supercooling was observed. The radial distribution functions inside those pockets show patterns typical of the liquid state. In addition, we calculated, by canonical molecular dynamics, the self-diffusion coefficients for some states. They were always on the order of 10^{-5} cm² s⁻¹, a magnitude consistent with a normal liquid phase.^{1,21}

The rise of the triple-point temperature from C_{60} to C_{84} reflects the increase in their potential depths (see Figures 1 and 4). This and the simultaneous effect of molecular size cause a relative dislocation of the phase diagrams to higher critical temperatures and lower densities.

As far as the critical- and triple-point pressures are concerned, it is expected that they should also significantly increase from C_{60} to C_{84} considering the rise in the temperature. The respective pressures for the different fullerenes are, however, on the same order of magnitude, which seems to reflect the relative decrease in the densities.

Regarding the critical- and triple-point properties in reduced units presented in Table 5, they seem to confirm that some kind of corresponding states rule may be established for fullerenes according to the suggestion of Abramo et al.¹ Incidentally, the reduced properties were directly obtained from the simulated results by the usual equations: $T^* = Tk_B/\epsilon$; $\rho^* = \rho R_0^3$; $p^* = p R_0^3/\epsilon$. In the next section, we shall report the reduced enthalpies of sublimation.

Overall, our results agree very well with those of Abramo et al.¹ However, the present simulated critical temperatures are lower than the ones worked out by them from the corresponding states rule. This also seems to be in accordance with their mentioned preliminary GEMC simulations of C_{84} . Moreover, the present results confirm the consistency of the MHNC theoretical approach.

4. Enthalpies of Sublimation

From the vapor–solid coexistence simulations, we worked out the enthalpies of sublimation as a function of temperature starting at the predicted triple points. They are displayed in Figure 5. The results for C_{60} have been reported elsewhere.⁹

TABLE 4: Critical- and Triple-Point Properties

		ρ_{cr}/nm^{-3}	T_{cr}/K	p_{cr}/bar	$\rho_{tr,liq}/\text{nm}^{-3}$	T_{tr}/K	p_{tr}/bar
C_{60}	ref 9	0.42 ± 0.01	1951 ± 28	33 ± 9	1.02 ± 0.01	1529 ± 36	4 ± 19
	ref 7	0.42	1941		1.00	1500	
C_{70}	this work	0.36 ± 0.03	2131 ± 44	29.5 ± 1.3	0.88 ± 0.01	1694 ± 49	4.44 ± 1.31
	ref 1	0.376	2140		0.88	1650	
C_{76}	this work	0.35 ± 0.03	2204 ± 59	32.5 ± 1.4	0.79 ± 0.01	1737 ± 34	4.41 ± 2.59
C_{84}	this work	0.29 ± 0.05	2293 ± 60	24.4 ± 1.6	0.69 ± 0.01	1884 ± 50	5.83 ± 2.19
estimates from the corresponding states rule							
C_{70}	ref 1	0.36	2190		0.85	1703	
C_{76}	ref 1	0.32	2284		0.77	1775	
C_{84}	ref 1	0.29	2448		0.68	1902	

TABLE 5: Triple- and Critical-Point Properties in Reduced Units

	ρ_{cr}^*	T_{cr}^*	p_{cr}^*	$\rho_{tr,liq}^*$	T_{tr}^*	p_{tr}^*
C_{60}	0.37 ± 0.01	0.60 ± 0.01	0.07 ± 0.02	0.90 ± 0.01	0.47 ± 0.01	0.01 ± 0.04
C_{70}	0.37 ± 0.04	0.58 ± 0.01	0.06 ± 0.01	0.90 ± 0.01	0.46 ± 0.01	0.01 ± 0.01
C_{76}	0.40 ± 0.04	0.58 ± 0.01	0.07 ± 0.01	0.91 ± 0.01	0.46 ± 0.01	0.01 ± 0.01
C_{84}	0.38 ± 0.07	0.56 ± 0.01	0.06 ± 0.01	0.89 ± 0.01	0.46 ± 0.01	0.01 ± 0.01

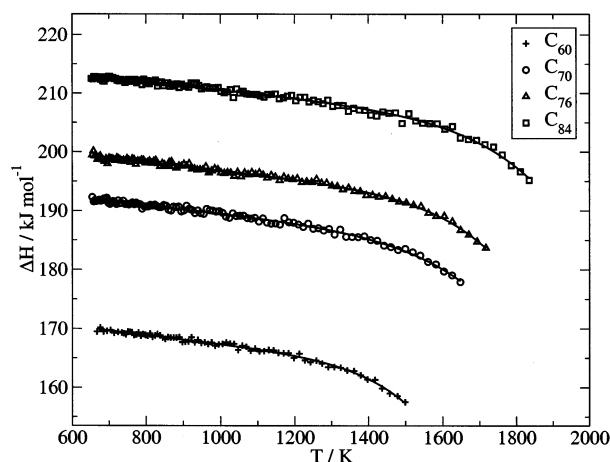


Figure 5. Enthalpies of sublimation as a function of temperature (solid lines indicate fits to eq 3).

TABLE 6: Enthalpies of Sublimation (kJ mol⁻¹)

	simulated results			experimental results		
	700 K	298 K	0 K	NIST ²³	Markov et al. ²⁴	
C ₆₀	170 ± 12	173 ± 12	174	176 ± 2	181 ± 2	175 ± 14
C ₇₀	191 ± 13	194 ± 13	196	196 ± 7	200 ± 6	
C ₇₆	198 ± 14	201 ± 14	203		206 ± 4	
C ₈₄	212 ± 15	215 ± 15	217		225 ± 6	

The simulation results were fitted to the following equation:²²

$$\Delta_{\text{sub}}H = ZRT^2 \frac{d \ln p}{dT} \quad (3)$$

with

$$\ln p = A + \frac{B}{T} + C \ln T + DT^E \quad (4)$$

Table 6 contains some numerical values. They are in very good agreement with the available experimental data.^{23,24} The enthalpies at 700 K (ΔH_{700}) were directly obtained from the simulated vapor–solid results. The standard (ΔH_{298}°) and third-law enthalpies (ΔH_0°) were estimated by an extrapolation of the simulation results and of the fitting lines to 298.15 and 0 K, respectively. The error bars, for the simulated results presented in Table 6, are the maxima of the standard deviations for the sublimation enthalpies of each fullerene at different temperatures.

An increase in the enthalpy of sublimation from C₆₀ to C₈₄ reflects, once again, the relative increase in their potential depths (see Figure 1). It is worth pointing out the relative variation in the enthalpy from C₆₀ to C₈₄. In fact, the differences between the potential depths (see Table 1) are $\Delta\epsilon/k_B(\text{C}_{70}-\text{C}_{60}) = 435$ K, $\Delta\epsilon/k_B(\text{C}_{76}-\text{C}_{70}) = 155$ K, and $\Delta\epsilon/k_B(\text{C}_{84}-\text{C}_{76}) = 273$ K. These differences clearly influence the relative location of the enthalpy curves (see Figure 5). The effect is also clearly visible in the critical- and triple-point regions of the phase diagrams (see Figure 4).

We also calculated, for example, the third-law sublimation enthalpies in reduced units. The value is 6.4 for all fullerenes, in excellent accordance with the corresponding states rule. Thus, taking the potential depth indicated by Abramo et al.¹ for C₉₆, we predict its third-law enthalpy of sublimation to be $\Delta H_0^\circ = 222$ kJ mol⁻¹.

Finally, the present results for the enthalpies of sublimation constitute a further test of the consistency of our method for

the determination of triple-point properties and suggest that at least these properties should approach those of real fullerenes.

5. Conclusions

We have presented a comparative study of the phase diagrams and enthalpies of sublimation of four model C_n fullerenes carried out strictly by computer simulation.

In view of the present results, the following general conclusions can be drawn. The liquid pockets for the studied fullerenes extend over ~450 K. No liquid supercooling was observed. The radial distribution functions and self-diffusion coefficients are consistent with a normal liquid phase.

There is a rise in the triple-point temperature from C₆₀ to C₈₄ due to the increase in the respective potential depths. This and the simultaneous effect of molecular size cause a relative dislocation of the phase diagrams to higher critical temperatures and lower densities. The respective critical- and triple-point pressures, however, are on the same order of magnitude, which seems to reflect the relative decrease in the densities.

Regarding the critical- and triple-point properties as well as the sublimation enthalpies in reduced units, the results seem to confirm that some kind of corresponding states rule may be established for fullerenes according to the recent suggestion of Abramo et al. On the basis of that, the sublimation enthalpy of C₉₆ is predicted.

Overall, our results, obtained strictly by computer simulation, are in good accordance with those of Abramo et al. from a combination of simulation and theory and confirm the consistency of the MHNC theoretical approach.

The enthalpies of sublimation are in excellent agreement with the available experimental data. There is an increase of the sublimation enthalpies from C₆₀ to C₈₄ due to the relative increase in the potential depths. The differences between the potential depths are also clearly reflected in the relative location of the phase diagram and enthalpy curves.

Because the calculation of the sublimation enthalpies started from the predicted triple points, it is suggested that at least the triple-point properties of the present model should approach those of real fullerenes. Considering that some experiments show that solid C₆₀ is unstable at ~1200 K, this suggestion may be confirmed or rejected only if there are any experimental means to prevent the decomposition of fullerenes.

Finally, we believe that the present results are valuable in two ways: first, they give an estimate of the phase diagrams of an important class of carbon forms, and second, they provide insight into the relation between thermodynamic properties and the underlying potential functions.

Acknowledgment. Fundação para a Ciência e a Tecnologia (FCT) is gratefully acknowledged for financial support. We are also thankful to Intel Corporation for free access to their compilers and to the GNU and Linux communities for the invaluable tools they offer.

References and Notes

- (1) Abramo, M. C.; Caccamo, C.; Costa, D.; Pellicane, G. *Europhys. Lett.* **2001**, *54*, 468.
- (2) Girifalco, L. A. *J. Phys. Chem.* **1991**, *95*, 5370. Girifalco, L. A. *J. Phys. Chem.* **1992**, *96*, 858.
- (3) Hasegawa, M.; Ohno, K. *J. Chem. Phys.* **1999**, *111*, 5955.
- (4) Cheng, A.; Klein, M. L.; Caccamo, C. *Phys. Rev. Lett.* **1993**, *71*, 1200.
- (5) Caccamo, C. *Phys. Rev. B* **1995**, *51*, 3387.
- (6) Caccamo, C. *Phys. Rep.* **1996**, *274*, 1.
- (7) Caccamo, C.; Costa, D.; Fucile, A. *J. Chem. Phys.* **1997**, *106*, 255.

- (8) Fartaria, R. P. S.; Fernandes, F. M. S. S.; Freitas, F. F. M.; Rodrigues, P. C. R. *Int. J. Quantum Chem.* **2001**, *84*, 375. Fartaria, R. P. S.; Fernandes, F. M. S. S.; Freitas, F. F. M.; Rodrigues, P. C. R. *Int. J. Quantum Chem.* **2002**, *88*, 355.
- (9) Fartaria, R. P. S.; Fernandes, F. M. S. S.; Freitas, F. F. M. *J. Phys. Chem. B* **2002**, *106*, 10227.
- (10) Pacheco, J. M.; Ramalho, J. P. P. *Phys. Rev. Lett.* **1997**, *79*, 3873.
- (11) Fernandes, F. M. S. S.; Fartaria, R. P. S.; Freitas, F. F. M. *Comput. Phys. Commun.* **2001**, *141*, 403.
- (12) Zubov, V. I.; Tretiakov, N. P.; Zubov, I. V. *Eur. Phys. J. B* **2000**, *17*, 629.
- (13) Hasegawa, M.; Ohno, K. *J. Phys.: Condens. Matter* **1997**, *9*, 3361.
- (14) Panagiotopoulos, A. Z. *Mol. Phys.* **1987**, *61*, 813.
- (15) Panagiotopoulos, A. Z.; Quirke, N.; Stapleton, M.; Tildesley, D. J. *Mol. Phys.* **1988**, *63*, 527.
- (16) Frenkel, D.; Smit, B. *Understanding Molecular Simulation: From Algorithms to Applications*; Academic Press: San Diego, CA, 1996.
- (17) Kofke, D. A. *J. Chem. Phys.* **1993**, *98*, 4149.
- (18) Agrawal, R.; Kofke, D. A. *Mol. Phys.* **1995**, *85*, 23.
- (19) Agrawal, R.; Kofke, D. A. *Mol. Phys.* **1995**, *85*, 43.
- (20) Stanley, H. E. *Introduction to Phase Transitions and Critical Phenomena*; Oxford University Press: New York, 1971.
- (21) Abramo, M. C.; Coppolino, G. *Phys. Rev. B* **1998**, *58*, 2372.
- (22) Diogo, H. P.; Santos, R. C.; Nunes, P. M.; Piedade, M. E. M. *Thermochim. Acta* **1995**, *249*, 113.
- (23) NIST Chemistry WebBook. <http://webbook.nist.gov>. Linstrom, P. J., Mallard, W. G., Eds.; NIST Standard Reference Database Number 69; July 2001; National Institute of Standards and Technology: Gaithersburg, MD.
- (24) Markov, V. Y.; Boltalina, O. V.; Sidorov, L. N. *Russ. J. Phys. Chem. (Transl. of Zh. Fiz. Khim.)* **2001**, *75*, 1.